

[Re] Multiple dynamical modes of thalamic relay neurons: rhythmic bursting and intermittent phase-locking

Georgios Detorakis¹

¹ Department of Cognitive Sciences, UC Irvine, CA, USA

gdetorak@uci.edu

Editor

Name Surname

Reviewers

Name Surname

Name Surname

Received Sep, 1, 2015

Accepted Sep, 1, 2015

Published Sep, 1, 2015

Licence [CC-BY](#)

Competing Interests:

The authors have declared that no competing interests exist.

 [Article repository](#)

 [Code repository](#)

A reference implementation of

→ *Multiple dynamical modes of thalamic relay neurons: rhythmic bursting and intermittent phase-locking*, Wang, X-J, Neuroscience, 59(1), pg. 21–31, 1994.

Introduction

This work introduces a reference implementation of a neuron model for thalamocortical relay neurons, proposed by X-J Wang, [4]. The model is conductance-based and takes advantage of an interplay between a T-type calcium current and a non-specific cation sag current and thus, it is able to generate spindle and delta rhythms. Another feature of this model is the presence of an intermittent phase-locking phenomenon where action potentials of sodium take place in a non-periodic manner, despite the fact that they are phase-locked to the periodic input current. Finally, the model is capable of generating tonic spike patterns. The source code of reference implementation is written in Python (Numpy, Scipy, Matplotlib, and Scikit-image).

Methods

In this section, a detailed description of the model is given following the paradigm of Nordlie et al, [3]. To this end description of the model, equations, parameters, and inputs are given in the form of tables.

Table 1 provides a description of the model, Table 2 provides information about simulations duration and temporal integration time steps, Table 3 gives a glimpse of the input signals used in this work. Table 4 introduces the equations of the model and finally Table 5 summarizes all the parameters for each figure (simulation). The neuron model is conductance-based consisting of four differential equations describing the dynamics of membrane potential and the kinetics of a T-Type calcium current, a Sag current channel and a Potassium channel. The rest currents are described by algebraic equations. The reference implementation has been done in a Python class (Python 3.5.1) along with Numpy (version 1.10.4), Scipy (version 0.17.0), Matplotlib (1.5.1) and Scikit-image (version 0.12.3). The numerical integration has been done using the *ode* method of Scipy *integrate* package. Three different methods have been tested in this work (*dopri5*, *Adams*, *BDF*, [1]). *Dopri5* is the closest numerical method to the one used by [4] (fifth-order adaptive size Runge-Kutta method). *BDF* and *Adams* provide similar numerical results as the first one, but they are faster. In

Model Summary	
Populations	No population – one neuron model
Topology	–
Connectivity	–
Neuron Model	Hodgkin-Huxley conductance-based
Channel Models	
Synapse Model	–
Plasticity	–
Input	Constant current or periodic rectangular pulses
Measurements	Membrane potential, channels activation, phase plane

Table 1: Summary of the model

the current implementation of [4] the user has the option to choose one of the three methods at the stage of class instantiating. All three aforementioned methods have been tested by comparing, spike times, amplitudes and the coefficient of variation using as threshold value 0 mV. Spike events were overlapping, and $CV \simeq 3.5$ for all three methods. A difference found in the amplitude of spikes generated by the three methods. Figure 1 shows two histograms of error distribution (error is defined to be the absolute difference of spike amplitude between two methods). Top histogram depicts a distribution of differences in amplitude between *dopri5* and *Adams* methods (gray color). The bottom histogram illustrates the distribution of amplitude differences between *dopri5* and *BDF* methods (red color). In the rest of the article all the results have been produced by using the *Adams* method.

Simulation Time		
Figure	Simulation Time (s)	Integration Step (ms)
1	6	0.05
2	$15 \times period, 5$	0.05
3	6	0.05
4	1.5, 1, 1	0.05
5	5	0.05
6	5	0.05
7	40, 20	0.05

Table 2: Simulations Time

All simulations ran on a Dell OptiPlex 7040, equipped with a sixth generation i7 processor, 8 GB of physical memory and running Arch Linux. The total execution time of all simulations was 526 minutes and the peak consumed memory was 465 MB¹. All the parameters used in this work are given in Table 5.

¹Python memory profiler used (https://pypi.python.org/pypi/memory_profiler).

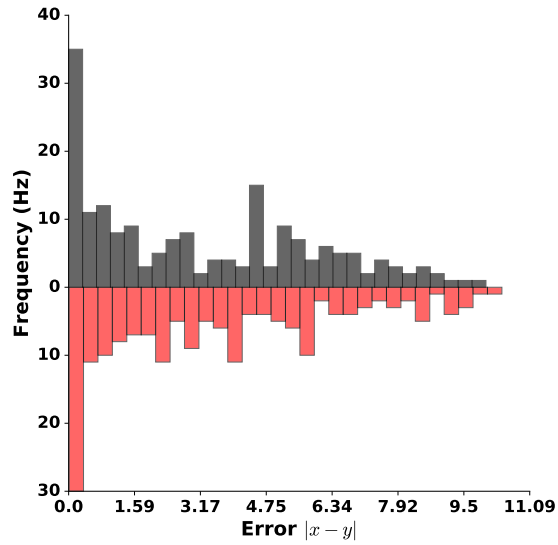


Figure 1: Amplitude difference distribution **Top histogram** depicts the distribution of differences in spikes amplitudes between *dopri5* and *Adams* integration methods of *Scipy integrate* package (black color). **Bottom histogram** illustrates the distribution of differences in spikes amplitudes between *dopri5* and *BDF* methods (red color). In both cases the number of bins is 30.


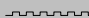

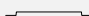



Figure	Type	Input			
		Form	Frequency ($\frac{1}{P_0}$, Hz)	Duration (p , ms)	Amplitude ($\mu\text{A}/\text{cm}^2$)
Figure 1	Constant		—	—	−0.6
Figure 2	Periodic		5, 10	10, 40	−1.0 +3.0 3 0.0 −0.45 −0.455 −0.47 −0.55 −0.6 −0.8 −1.3 −1.4 −2.1 −1.25
Figure 3	Constant		—	—	0.25
Figure 4	Pulse/Constant		—	100	−0.47 −0.95
Figure 5	Constant		—	—	[−2, 0]
Figure 6	Constant		—	—	[−2, 0]
Figure 7	Constant		—	—	[−2, 0]

Table 3: Description of the applied current I_{app}

Neuron Model	
Name	Thalamocortical relay neuron
Type	Conductance-based neuron
Membrane Potential	$C_m \frac{dV(t)}{dt} = -I_T - I_h - I_{Na} - I_K - I_{Na(P)} - I_L + I_{app}$
T-Type Calcium Current (I_T)	$I_T = g_T \cdot s_\infty^3(V) \cdot h \cdot (V - V_{Ca})$
	$s_\infty(V) = \frac{1}{1 + \exp(-\frac{V+65}{7.8})}$
	$\frac{dh(t)}{dt} = \phi_h \frac{h_\infty(V) - h}{\tau_h(V)}$
	$h_\infty(V) = \frac{1}{1 + \exp(\frac{V-\theta_h}{k_h})}$
	$\tau_h(V) = h_\infty \exp(\frac{V + 162.3}{17.8}) + 20$
Sag Current (I_h)	$I_h = g_h \cdot H^2 \cdot (V - V_h)$
	$H_\infty(V) = \frac{1}{1 + \exp(\frac{V+69}{7.1})}$
	$\frac{dH(t)}{dt} = \phi_H \frac{H_\infty(V) - H}{\tau_H(V)}$
Hodgkin-Huxley Currents (I_K) and (I_{Na})	$I_K = g_K \cdot n^4 \cdot (V - V_K)$
	$\frac{dn(t)}{dt} = \phi_n \frac{n_\infty(V) - n(t)}{\tau_n(V)}$
	$n_\infty(\sigma_K, V) = \frac{\alpha_n(\sigma_K, V)}{\alpha_n(\sigma_K, V) + \beta_n(\sigma_K, V)}$
	$\tau_n(\sigma_K, V) = \frac{1}{\alpha_n(\sigma_K, V) + \beta_n(\sigma_K, V)}$
	$\alpha_n(\sigma_K, V) = \frac{-0.01(V + 45.7 - \sigma_K)}{\exp(-0.1(V + 45.7 - \sigma_K)) - 1}$
	$\beta_n(\sigma_K, V) = 0.125 \exp(-\frac{V + 55.7 - \sigma_K}{80})$
	$I_{Na} = g_{Na} \cdot m_\infty^3(\sigma_{Na}, V) \cdot (0.85 - n) \cdot (V - V_{Na})$
	$m_\infty(V) = \frac{\alpha_m(\sigma_{Na}, V)}{\alpha_m(\sigma_{Na}, V) + \beta_m(\sigma_{Na}, V)}$
	$\alpha_m(\sigma_{Na}, V) = -0.1 \frac{V + 29.7 - \sigma_{Na}}{\exp(-0.1(V + 54.7 - \sigma_{Na})) - 1}$
	$\beta_m(\sigma_{Na}, V) = 4 \exp(-\frac{V + 54.7 - \sigma_{Na}}{18})$
Persistent Sodium Currents ($I_{Na(P)}$)	$I_{Na(P)} = g_{Na(P)} \cdot m_\infty^3(\sigma_{Na(P)}, V) \cdot (V - V_{Na})$
Leak Current (I_L)	$I_L = g_L \cdot (V - V_L)$

Table 4: Description of the neuron model

Model Parameters							
Figure	V_0 (mV)	g_T (mS/cm ²)	θ_h (mV)	k_h (mV ⁻¹)	σ_{Na} (mV)	g_L (mS/cm ²)	V_L (mV)
1	-74	1	-79	-5	6	0.12	-70
2	-74	1	-81	6.25	3	0.1	-72
3	-74	0.3	-79	5	6	0.12	-70
4	-72/-64	1.0	-79	5	6	0.12	-70
5	-74	0.3	-75	5	6	0.08	-70
6	-74	1/0.7	-79	5	6	0.1/0.04	-70
7	-72	0.3/0.25	-81	6.25	3	0.1	-72
Common Parameters							
$C_m = 1 \mu\text{F/cm}^2$, $\phi_h = 2$, $V_{Ca} = 120 \text{ mV}$, $\phi_H = 1$, $g_h = 0.04 \text{ mS/cm}^2$, $V_h = -40 \text{ mV}$, $g_K = 30 \text{ mS/cm}^2$, $V_K = -80 \text{ mV}$, $g_{Ca} = 42 \text{ mS/cm}^2$, $V_{Ca} = 55 \text{ mV}$, $\phi_n = 28.5$, $\sigma_K = 10 \text{ mV}$, $V_{Na(P)} = 55 \text{ mV}$, $\sigma_{Na(P)} = -5 \text{ mV}$, $g_{Na(P)} = 9 \text{ mS/cm}^2$							

Table 5: Simulation Parameters

Results

We simulated the model described in Table 4 using the parameters given in Table 5 and the corresponding input (see Table 3). First, we examined what is the response of the reference implementation to rhythmic hyperpolarization. In [4] this is illustrated in Fig 1². Thus, we applied a periodic current pulse of $-1 \mu\text{A}/\text{cm}^2$ amplitude at several different frequencies ($\frac{1}{P_0}$ is the frequency in Hz and P_0 is the corresponding period in ms) ranging from 0.1 Hz to 15 Hz with a resolution (discretization) of 100 points. The same number of samples used for discretizing the duration of the pulse for each frequency.

Upper panel shows two different simulations of the reference implementation at specific frequencies (5, 0.5 Hz) and ratios p/P_0 (0.6, 0.6), respectively (following the upper panels of Fig 1 in [4]). These panels are comparable to the ones presented in [4] and the timescales are exactly the same (400 ms for the left sub-panel and 4 s for the second one). However, numbers regarding pulse ON duration (p) in Fig 1 of [4] are not correct. For instance, take the frequency to be $\frac{1}{P_0} = 5 \text{ Hz}$ and $\frac{p}{P_0} = 0.6$ then the pulse ON duration must be $p = 120 \text{ ms}$ and not 160 ms.

Bottom panel illustrates the total results of the 100×100 simulations we ran. In order to create this figure, we counted the number of spikes generated per pulse, both supra-threshold and sub-threshold, and then we computed the mean (this procedure is not described in a solid way in [4], however it is described in [2]). This figure is different from [4], where the shaded area that contains an average number of spikes below 1.0 (but not zero) is larger than in [4]. Unfortunately, information regarding Fig 1 is limited in [4] in order to be able to follow a specific recipe and try to reproduce exactly the same figure.

Then we tested the transition from subthreshold to bursting oscillations via chaos. Therefore, we used a steady current varying only its amplitude keeping all the other parameters fixed. We used eight different values (exactly the same as in [4]),

$$I_{\text{app}} = 3.0, 0.0, -0.45, -0.455, -0.47, -0.55, -0.6, -0.8, -1.3, -1.4, -2.0 \mu\text{A}/\text{cm}^2.$$

Results are depicted in Figure 3. This figure corresponds to Fig 3 of [4]. In this case, there was no difference between the reference implementation and the original one.

The next simulation we performed reproduces results related to hysteresis as in Fig 4 of [4]. First, we run a simulation where the input current I_{ext} varied from $-0.433 \mu\text{A}/\text{cm}^2$ to $-0.55 \mu\text{A}/\text{cm}^2$. At every iteration, we detected if there is sub-threshold and/or suprathreshold activity in the membrane voltage trace. Thus we created the hysteresis diagram given in Figure 4, top panel. In addition, we tested the bistability of the current model using the same protocol as in [4]. According to that protocol, we first apply a brief pulse (for 100 ms) of $0.25 \mu\text{A}/\text{cm}^2$ and $-1.2 \mu\text{A}/\text{cm}^2$ followed by a steady current at $-0.47 \mu\text{A}/\text{cm}^2$. This causes the state of the model to switch from a purely subthreshold activity pattern to a mixed sub- and suprathreshold activity pattern. The results are given in Figure 4, right panel.

Another interesting behavior of the model is the development of a “spiral” chaos (see Fig 6 in [4]). The reference implementation is capable of generating similar behavior as Figure 5 shows. In order to get these results we applied a constant external current with an amplitude of $-0.95 \mu\text{A}/\text{cm}^2$.

The next simulation investigates how the bursting frequency is affected by the injected external current (see Fig 7 in [4], two bursting modes). To address this issue we captured data³ values for the external current from Fig 7 of the original article (dots in Fig 7, pg. 27 in [4]) using a software called PlotDigitizer⁴. The results from our simulations are illustrated in Figure 6. Black curve represents the

²From now and then original article's figures will be referred as Fig

³Data are available in the accompanying github repository of the present article.

⁴(<http://plotdigitizer.sourceforge.net/>)

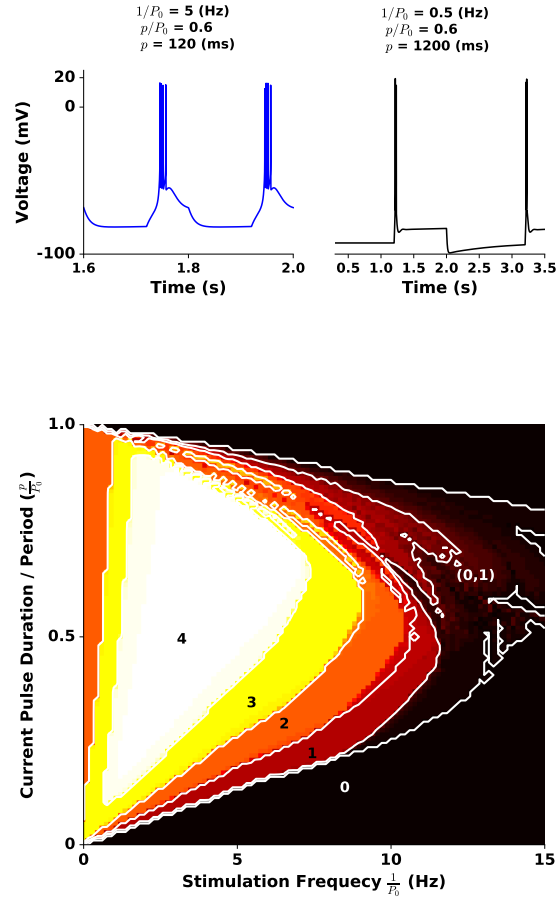


Figure 2: Responses to rhythmic hyperpolarizations. We stimulate the model with a periodic pulse with varying frequency $\frac{1}{P_0}$ in $[0.1, 15]$ Hz and ON pulse duration p . **Upper panels** Show the results of two specific simulations out of the 100×100 we ran in total. The blue curve illustrates a case where bursts of four spike take place when frequency is $\frac{1}{P_0} = 5$ Hz and $\frac{p}{P_0} = 0.6$. Black curve depicts a case of two spikes bursts. In this case the frequency is $\frac{1}{P_0} = 0.5$ Hz and $\frac{p}{P_0} = 0.6$. **Bottom panel** shows a range of frequencies $\frac{1}{P_0}$ from 0.1 Hz to 15 Hz versus the ratio $\frac{p}{P_0}$ in range $[0, 1]$. Numbers indicate the average number of spikes per pulse.

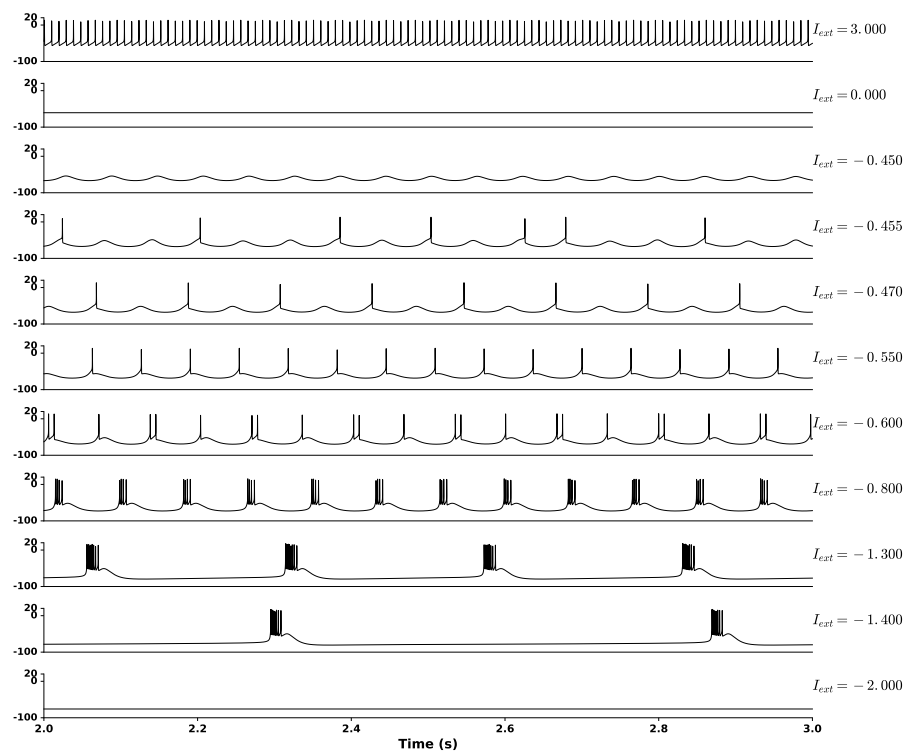


Figure 3: Dynamic behavior of neuron. Here we simulate the model with parameters given in Table 5. The only parameter that varies from panel to panel in this figure is the external current I_{ext} . These results correspond to Fig 3 of [4].

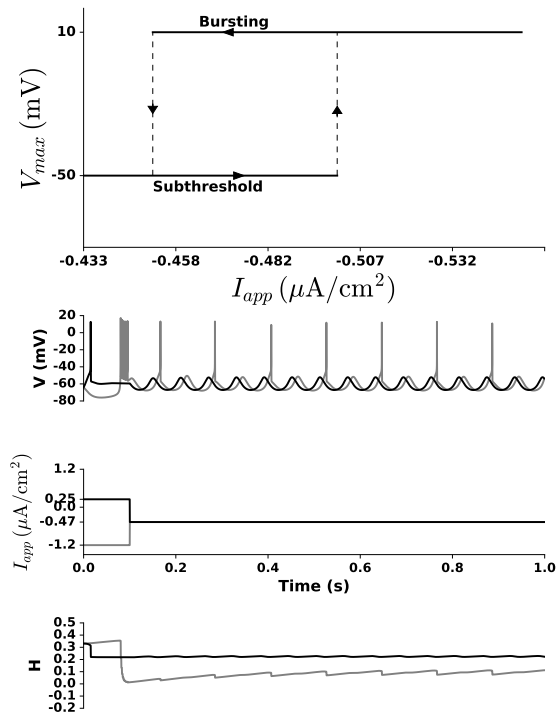


Figure 4: Hysteresis near the transition from the subthreshold to bursting oscillation. First panel: Hysteresis diagram indicates a coexistence of bursting and subthreshold activity. **Second panel:** Bistability example shows how the same system can produce either subthreshold activity (black curve) or burst activity (gray curve). **Third panel:** shows the activation of H for the same simulation as in the upper panel. **Fourth panel:** Input to the model for this simulation is a brief current pulse at $0.25 \mu\text{A}/\text{cm}^2$ (black curve) and $-1.2 \mu\text{A}/\text{cm}^2$ (gray curve) followed by a steady current at $-0.47 \mu\text{A}/\text{cm}^2$ for both simulations.

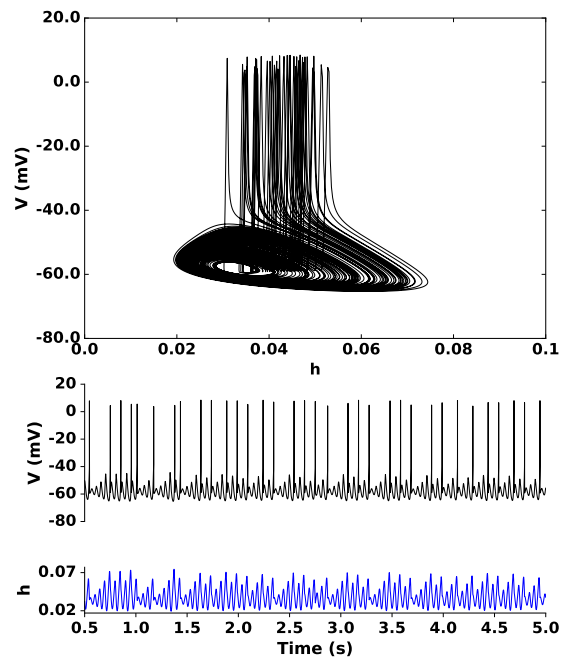


Figure 5: “Spiral Chaos”. In this Figure we show that the model is capable of generating “spiral chaos” as it has been shown in Fig 6 in [4]. The external current in this simulation is constant ($-0.95\mu\text{A}/\text{cm}^2$). **Top panel** shows the phase portrait of the membrane potential and the Sag current (V vs h). **Middle panel** illustrates the membrane potential (V) and, the **bottom panel** shows the h current over time.

frequency in Hz and the blue one the period in sec. Black dots indicate frequency and open circles the corresponding period (reference implementation), respectively. Cyan crosses show the original data taken from [4] and magenta pentagons the corresponding period. The original points and the reference implementation share a similar shape (and smoothness). However, there is a slight divergence for a few of the points.

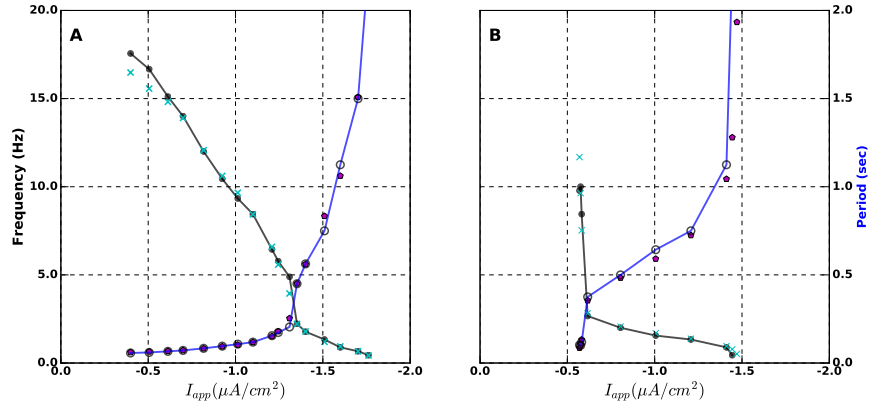


Figure 6: Frequency and period versus steady input current. This figure illustrates how the external current (ranging from 0 to $-2 \mu A/cm^2$ affects the bursts frequency (bursting mode) of the model. Black curve indicates frequency (black dots) in Hz and blue curve period (white circle discs) in sec. Cyan crosses (frequency) and magenta pentagons (period) indicate original data taken from [4].

The last simulation is related to Fig 2 of [4] and to an “intermittent” phase-locking phenomenon. A periodic pulse with frequency 10 Hz and ratio $\frac{P}{P_0} = 0.8$ is applied to the model as external input current. The response of the model is registered and sub- and supra-threshold spikes are counted. We applied six different current amplitudes and two different values for the T-type calcium conductance. $I_{app} = -1.4, -1.5, -1.6 \mu A/cm^2$ and $g_T = 0.3 mS/cm^2$ $I_{app} = -1.2, -1.5, -1.8 \mu A/cm^2$ and $g_T = 0.25 mS/cm^2$. Figure 7 shows 2 seconds of membrane potential along with symbolic patterns of 0 (dark circles) and 1 (green line segments). Results given in Figure 7 are similar to the ones of Fig 2A and Fig 2B in [4].

Conclusion

A conductance-based model for relay thalamocortical neurons proposed by [4] was implemented in Python. The model tested thoroughly in several examples taken from the original article. In general, the original model was easy to be implemented since all the equations and the most of the parameters (except the initial time step of the integration method) are given. The reference implementation results are similar to the original ones except maybe of Figure ?? (Fig 1 of [4]), where we found some divergence from the original results. Furthermore, not any other implementation of [4] found in order to be compared with the current reference implementation.

References

- [1] Uri M Ascher and Linda R Petzold. *Computer methods for ordinary differential equations and differential-algebraic equations*. Vol. 61. Siam, 1998.
- [2] DA McCormick and HR Feuser. “Functional implications of burst firing and single spike activity in lateral geniculate relay neurons”. In: *Neuroscience* 39.1 (1990), pp. 103–113.

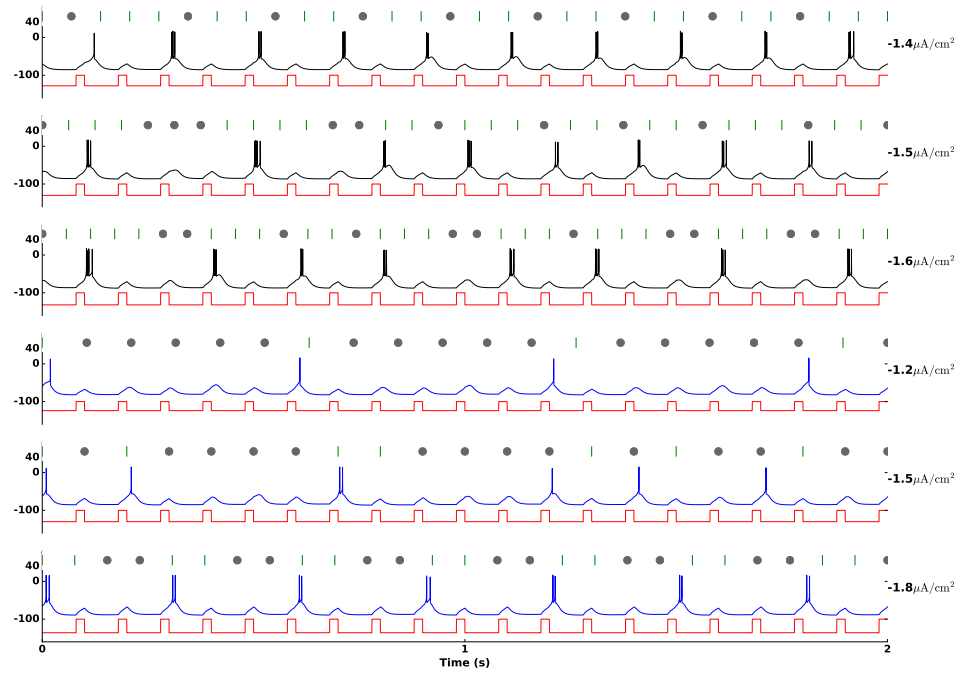


Figure 7: Symbolic patterns. Six different simulations are illustrated here ($I_{app} = -1.4, -1.5 - 1.6 \mu A/cm^2$ with $g_T = 0.3 mS/cm^2$) and ($I_{app} = -1.2, -1.5, -1.8 \mu A/cm^2$ with $g_T = 0.25 mS/cm^2$). Symbolic patterns are illustrated above membrane potential traces as green line segments – suprathreshold spikes and dark circles – subthreshold spikes. Red curve indicates the input periodic pulses.

- [3] Eilen Nordlie, Marc-Oliver Gewaltig, and Hans Ekkehard Plesser. "Towards reproducible descriptions of neuronal network models". In: *PLoS Comput Biol* 5.8 (2009), e1000456.
- [4] X-J Wang. "Multiple dynamical modes of thalamic relay neurons: rhythmic bursting and intermittent phase-locking". In: *Neuroscience* 59.1 (1994), pp. 21–31.